JOURNAL OF OPTOELECTRONICS AND ADVANCED MATERIALS Vol. 9, No. 7, July 2007, p. 2046 - 2055

Study of optical absorbtion spectra of manganese phosphate glasses doped with rare-earth oxides

SANAA M. EL-RABIE
Phys. and Maths. Dept., Faculty of Electronic Engineering Menoufia Univ. Menouf, Egypt.

Optical absorption spectra are recorded in the wavelength range from 200-1100 nm for $Mn(PO_3)_4$.x R.E where x = 0.25, 0.5, 1, 2, 4, 6 and 8 wt. % and R.E refers to one of the rare-earth oxides, (Nd_2O_3, Gd_2O_3 and Pr_6O_{11}) respectively. Optical absorption bands due to intra-configuration transition of R E elements are observed with their numbers, intensities and positions depend on the kind and concentration of the doped oxide. The optical energy gap, $E_{opt.}$, and the width of the band tail, ΔE, were calculated and their composition dependence was investigated and confirmed the appearance of 3-composition region which was obtained from density and molar volume data of worked glasses.

(Received April 5, 2007; accepted June 27, 2007)

Keywords: Optical absorption, Optical glass, Manganese phosphate glass, rare-earth doping

1. Introduction

In the last two decades, rare earth ion-doped solid media were used for developing several types of solid state lasers [1 - 4], and the optical properties of phosphate glasses with different transition metal doped with rare-earths are studied [5-9]. However, the effects of co-dopants ion clustering and site-to-site variation in the local field on the optical spectra and lasing properties of rare earth ions in glassy hosts have been surveyed [10]. The optical spectra of rare-earth ions are characterized by absorption bands, which are very sharp almost line like. These sharp bands are due to forbidden transitions involving the 4F levels which are allowed by electric dipole effects, and these 4F orbitals are very effectively shielded from interaction with external forces by the overlying $5S^2$ and $5P^6$ shells. Hence the states arising from the various $4F^{14}$ configuration are only slightly affected by the surroundings of the ions and remain practically invariant for a given ion in the various compounds. Therefor, in general, the rare-earth elements do not change the limits of the ultra-violet absorption edge of the base glass. The spectra of the rare earths reflect the stability of the empty, half-filled and filled 4F levels [11].

There are a number of characteristics, which distinguish glass from other solid laser host materials. Their isotropic character possibility of even heavy doping with excellent uniformity and the strong sharp fluorescence lines observed in rare-earth doped glasses make them host materials of choice for optically pumped laser device.

The crystal-field parameter calculations in oxide hosts consider the interaction between lanthanide 4F orbitals and the S and P orpitals of the ligands. Since the 4F levels can always be considered as localized, even in solids presenting very narrow energy gap, covalency is generally introduced as a phanomenological parameter in crystal field calculations. Optical transitions of a rare-earth ion in a solid matrix occur between states belonging to the same configuration $4F^n$ ($4F^2$, $4F^3$ and F^7 for Pr^{3+}, Nd^{3+} and Gd^{3+} respectively), which are forbidden by the Laporte rule because they involve states with the same parity [12].

The optical spectra of Nd^{3+} doped to different crystals and glasses were analyzed [6-8, 13]. The optical properties of Nd^{3+} doped phosphate glasses with various alkali and alkaline earth ions as network modifiers were investigated [14, 15]. These results indicated that the effect of an alkaline earth oxide depends on its ionic field strength and that the substitution of alkaline earth oxides with Nd_2O_3 lossens the glass structure as well as decreases the degree of disorder of the phosphate chain structure.

The promising transitions in Nd^{3+} ions in realizing laser action in phosphate glasses of various chemical compositions were investigated [16]. However, the reported results revealed the potential of the four transitions in Nd^{3+} ion ($^4F_{3/2} \rightarrow {}^4I_{11/2}$, $^4I_{9/2}$, $^4I_{13/2}$, $^4I_{15/2}$) in decreasing order, in integrated absorption cross-section for exhibiting laser action in the investigated glassy materials.

The measurements of the optical absorption coefficient particularly near the fundamental absorption edge provide a standard method for the investigation of optically induced electronic transitions and provide some ideas about the band structure and energy gap in both crystalline and non-crystalline materials [11].

The present work is devoted to the investigation of the effect of RE oxides content in $Mn(PO_3)_4$ .x RE glasses where x = 0.25, 0.5, 1, 2, 4, 6 and 8 wt.%, on the absorption spectra and their structure in the wavelength range of from 200 - 1100 nm.

2. Experimental technique

2.1. Glass preparation

Manganese-phosphate glasses containing rare-earth oxides were prepared from laboratory reagent grades of

composition: 50 mol% (MnO_2), 50 mol% (P_2O_5) and xwt% of (RE, rare-earth oxides), where x is 0.25, 0.5, 1, 2, 4, 6, and 8 wt%. The R.E. oxides are Pr_6O_{11}, Nd_2O_3 and Gd_2O_3. Melting of the glasses which were placed in recrystallized alumina crucible was done in an electrically heated furnace open to the atmosphere. The weighed quantities of these reagents in appropriate proportions were thoroughly mixed in the crucible and placed in an electric furnace held at 350 ^{0}C for one hour. This allowed the P_2O_5 to decompose and react with other batch components before melting would ordinarily occur. After this treatment, the mixture was placed in an another furnace held at 1000~1100 ^{0}C for one hour, with the highest temperature being applicable to the mixture richest in R.E. The glass melt was stirred from time to time using an alumina rod to ensure homogeneity. The melt was cast into a clean two mild-steel mould heated at 200 ^{o}C to form glass discs of 0.3 cm thickness and 1.6 cm diameter. The disc was immediately transferred to another annealing furnace, which was already set at 250 ^{0}C for one hour. This furnace was then switched off and the glasses were allowed to cool inside it to room temperature. After that, the glass samples were polished using alumina powder of grain size 0.1-1 μm where the thickness of glass samples are 0.6-1 mm.

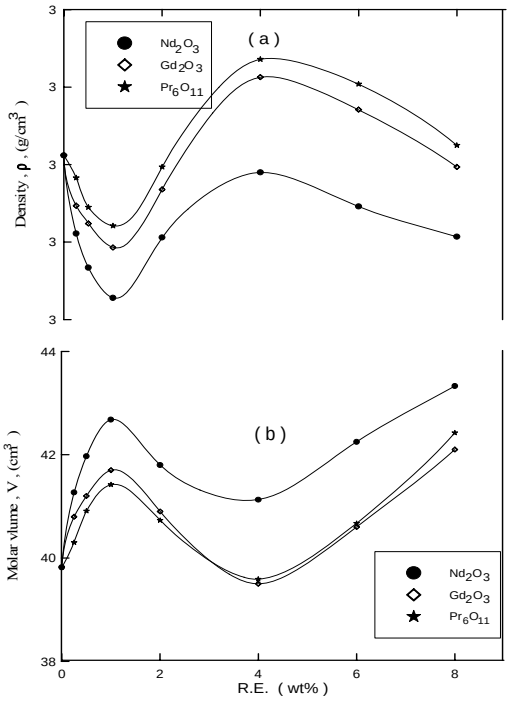

Fig. 1. Variation of (a) density ρ (gm/cm^3) and (b) Molar volume (cm^3) with RE wt % of $Mn(PO_3)_4$-$_X$ Re glasses (where RE are Nd_2O_3) or Gd_2O_3 or Pr_6O_{11}).

2.2 Measurements

The densities of the samples were measured by the Archimedes method using toluene as the immersion liquid and they are accurate to ±0.001 gm cm^{-3}. Absorption spectra of prepared glasses were recorded at room temperature by using a Perkin-Elmer lambda 4B UV / VIS spectrophotometer in the wavelength region 200~1100 nm.

3. Results and discussion

3.1 Compositional dependence of the glass density and molar volume on the rear earth oxides content

Fig. 1(a and b) shows the variations of the density and molar volume of prepared Mn $(PO_3)_4$. x R.E (where x = 0.25, 0.5, 1 , 2 , 4 , 6 and 8 wt.% and R.E refer to rare earth oxides content which are Nd_2O_3, Pr_6O_{11} and Gd_2O_3) glasses with the doped R.E oxides content. This figure shows a converse change in behavior of the compositional dependence of both the density and molar volume with two inflexion points around 1 and 4 wt.% of the R.E oxide content. This anomalous behavior of density and molar volume may be related to the changes in atomic masses, ionic (or atomic) size, cross-linking densities and occupied positions of the constituent elements in glasses [17-20].

The rare earth ions occupied the center of a distorted cube in glass, which is made of four tetrahedra of phosphate glasses so each tetrahedron contributes two oxygens to the coordination number of the rare earth ions which is 8 for the most rare-earth oxides as Reisfeld [19], and Brachjkovskaya et al. [20] reported that for rare-earth cation plays the role of a network cation modifier in meta-phosphate glasses. Also, it has been reported [21] that addition of Nd_2O_3 to the meta-phosphate glasses, pyro-phosphate glass phase appeared in the melt due to the reaction:

$$Nd_2O_3 + 3Mn(PO_3)_4 \rightarrow 3\ MnP_2O_7 + 2\ Nd(PO_3)_3 \quad (1)$$

The amount of pyro-phosphate glass appeared to be proportional to the amount of R.E. oxide added.

As mention before, the rare earth ions may inter the glass network interstitially. So some network bonds, P-O-P and Mn-O-P are broken and replaced by ionic bonds between rare-earth ions and singly bonded oxygen atoms. These broken network bonds will cause an increases in the molar volume and consequently decreases in the values of density in the first glass region (0 to 1 wt% (RE) oxides content).

By addition of rare earth oxides to the studied glasses systems leads to an increase in cross-linking, which may be attributed to the continuously filling up the vacancies amidst the network by interstitial rare-earth ions which increase in the rigidity in the glass structure with increaseing the concentration of the modifying oxide signifies [22], i.e. the P-O-P and Mn-O-P are broken with

the addition of modifying oxide, giving singly bonded oxygen atoms and providing an excellent example of the Zachariasen network theory [23]. So that the glass density increased in the compositional region (1-4 wt%) rare-earth content (of atomic masses 144.24, 157.25 and 140.91 for Nd, Gd and Pr respectively) which causes an increase of the packing density and will reduce the averged interatomic spacing, which decreases the molar volume (see Fig. 1 (a and b) from the range 1-4wt.%.

Also, one may expect that the addition of R.E. oxide to the studied glass system leads to an increase in cross-link density (cross-link densities of P, Mn in meta-phosphate, Mn in pyro-phosphate and R.E. are 2, 2, 4, and 6, respectively). So the observed increases in the density and decreases in the molar volume in the second compositional region (1-4 wt.%) may be probably attributed to the effect of adding Nd cations of atomic mass 144.24, 157.25 and 140.91 for Nd, Gd and Pr respectively and cross-link density 6 for each kind of the R.E. oxides, and changing the cross-link density of Mn cation to 4 in pyro phosphate which are greater than those for P and Mn of atomic masses 30.97, 54.94 and cross-link density of 2, 2 in meta-phosphate, respectively.

Finally, in the third compositional region (4-8 wt% (RE) oxides content) the glass density decreases and the molar volume increases. This indicate that the rare-earth ions may be enter the glass network interstitially [19]. Hence the decrease due to a structural change in the glass network may be some network bonds P-O-P are broken and repleced by a weak ionic bonds between rare-earth ions and singly bonded oxygen atoms, then an increase in the molar volume and a consequent a decrease in the desity values with increasing rare earth oxides content would be expected from 4-8 wt.% (see Fig. 1 (a and b)).

However, the curves indicating that the density/molar volume variations with the wt% of R.E. oxide for Gd_2O_3 are lying between those of the lower curves for Nd_2O_3 and the upper ones corresponding to Pr_6O_{11}. This observed dependence of density/molar volume levels variations with the type of R.E. oxide may be attributed to the differences of the molecular weights of these studied R.E. oxides (Their molecular weight values are 1021.4, 362.5 and 336.5 for Pr_6O_{11}, Gd_2O_3 and Nd_2O_3, respectively) and the differences of their ionic radii (0.92 Å, 1.02 Å and 1.08 Å respectively). Therefore, for the glasses containing Pr_6O_{11} contents, their density values are the highest and those corresponding to glasses containing Nd_2O_3 their density values are the lowest as expected and vice versa for the values of their molar volumes. However, glasses containing Gd_2O_3 have their density and molar volume values lying between the density/molar volume values of these glasses containing other RE oxides.

3.2. Absorption spectra for $Mn(PO_3)_4$. x R.E. glasses

Fig 2 (a, b and c) shows the absorption spectra in the region, 200-1100 nm (i.e. UV and VIS. ranges) as were recorded at room temperature for all manganese-phosphate glasses doped with Nd_2O_3, Gd_2O_3 and Pr_6O_{11} oxides respectively. The illustrated spectra in this figure are dependent on the type of the doped R.E. oxide. However, for all glasses, doped with the same R.E. oxide, the spectra are, in general, similar in character in that, the number of absorption peaks is the same but their intensities are increased with the increase of the wt% of the doped RE oxide content in the glass. Anyhow, the number of observed peaks are 8, 3 and 5 for the cases of Nd_2O_3, Gd_2O_3 and Pr_6O_{11} oxides in the above figure, respectively.

Inspection of the above Fig. 2 (a, b and c) reveals also that, the absorption spectra for all samples show that there is a broad band occurred nearly in the range of wavelengths, 550-570 nm. This band may be due to the presence of Mn^{+2} and Mn^{+3} ions in tested glasses, where it has been reported [24] that manganese ions produce absorption peak at 541 nm and another stronger one at 500 nm during the investigation of optical properties of MnO-CeO-P_2O_5 glass. Also it has been found that, the crystalline system MnO-ZnO doped with RE oxides [25] showed three characteristic absorption peaks at 610, 480 and 420 nm due to the presence of Mn^{+2} ion.

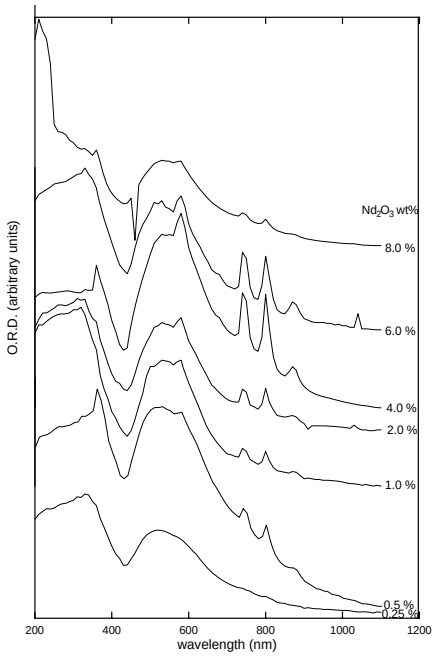

Fig. 2. (a) The uv-vis optical absorption spectra for the studied $Mn(PO_3)_{4-X}Nd_2O_3$ glasses.

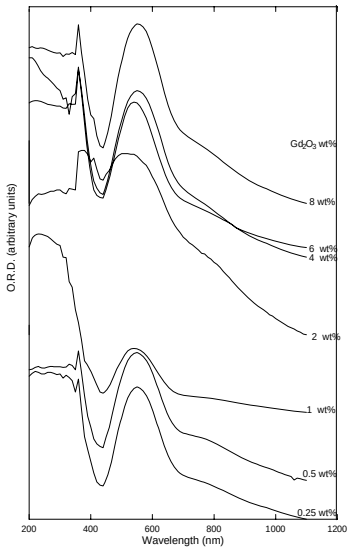

Fig. 2. (b) The uv-vis optical absorption spectra for the studied $Mn(PO_3)_2$.x Gd_2O_3 glasses.

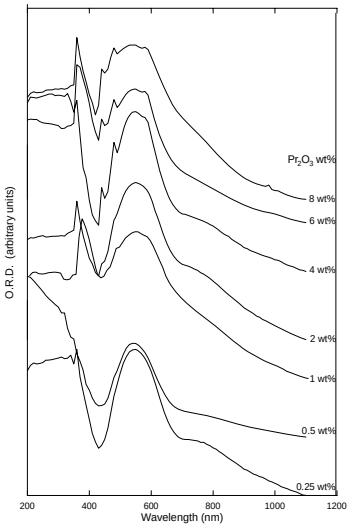

Fig. 2. (c) The uv-vis optical absorption spectra for the studied $Mn(PO_3)_2$.x Pr_6O_{11} glasses.

K. Binnemans [26] reported that the transitions observed in the absorption spectra of the trivalent lanthanide ions are intraconfigrational F-F transitions, where lanthanide ions may give rise to sharp absorption peaks [27], where electrons responsible for the spectral and magnetic properties of lanthanide ions are 4F electrons, and the 4f orbitals are very effectively shielded from interaction with external forces by overlying $5S^2$ and $5P^6$ shells. Hence the states arising from the various $4F^n$ configuration are only slightly affected by the surroundings of the ions and remain practically invariant for a given ion in various compounds, the majority of these transitions are induced electric dipole transitions. These transitions through normally dipole forbidden, become allowed in the glassy host [28] due to vibronic interaction or through admixture of add electric wave-function. In the free ion state these transitions are prohibited by the parity rule of electronic dipole transitions [29]. However, this prohibition can be avoided by ions embedded in a crystal field by non-centrally symmetric interaction of the ions with the surrounding ions which mix state of opposite parity and thus relax the parity restraction.

However, the other absorption lines in Fig. 2 (a, b and c) of tested glasses interpreted similarly as interpreted by A.H. Khafagy et.al. [30], for the absorption spectra of zinc-phosphate glasses doped with Nd_2O_3 R.E oxide. Then, the observed absorption spectra of the present tested manganese-phosphate glasses are attributed to the intra-configurational electronic transitions within the 4F shell of RE ions [19], which are only affected by the surrounding ions and remain practically invariant for a given ion in various compounds, which illustrated as follows

3.2.1. Nd^{3+} ($4F^3$)

Optical properties for Nd^{3+} has been investigated by several authors [3, 13, 16, 30 and 31]. The transitions for Nd^{3+} ion occur from the $^4I_{9/2}$ ground state level to other excited levels [31], Accordingly, the transition wavelengths with their corresponding assignments and the peaks of the absorption coefficient $\alpha_{max.}$ are given in Table 1. From this Table, it is clear that the transitions occurr between $^4I_{9/2}$ and $^4F_{3/2}$, $^4F_{5/2}$ or $^4H_{9/2}$ or $^4S_{3/2}$, $^4F_{9/2}$ or $^4G_{5/2}$, $^2G_{7/2}$ or $^4G_{7/2}$,$^4G_{9/2}$, $^2K_{13/2}$ or $^4G_{11/2}$ or $^2D_{3/2}$,$^2K_{15/2}$ or $^4P_{1/2}$,$^2D_{5/2}$ levels.

Table 1. Absorption spectra of Nd^{3+} in $Mn(PO_3)_2$.x Nd_2O_3 glasses.

Observed Transitions	Wavelength (nm)	$\alpha_m(cm^{-1})$ for glasses with different values of x						
		0.25%	0.5%	1 %	2 %	4 %	6 %	8 %
$^4I_{9/2} \rightarrow {}^4F_{3/2}$	874		0.3080.7380.769	0.5	0.6241.74	1.44	1.5584.53	1.6464.7
$\rightarrow {}^4F_{5/2}$, $^2H_{9/2}$	802		2.4312.6311.646	1.071.2	1.7114.29	3.98	.9526.422	4.3256.75
$\rightarrow {}^4F_{9/2}$, $^4S_{3/2}$	745		2.8152.98	42.5	14.4712.4	3.77	6.5744.25	46.9634.5
$\rightarrow {}^4G_{5/2}$, $^2G_{7/2}$	583			2.712.0	913.12	5.96	67.2167.6	217.7
$\rightarrow {}^4G_{7/2}$, $^4G_{9/2}$, $^2K_{13/2}$	535	2.2		92.743.	3.62	5.36	76	7.98
$\rightarrow {}^4G_{11/2}$	408	1.71		26		2.97		
$\rightarrow {}^2D_{3/2}$, $^2K_{15/2}$	352	2.79				4.95		
$\rightarrow {}^4P_{1/2}$, $^2D_{5/2}$	331	2.79				5.1		

Also, the values of the absorption coefficient corresponding to these absorption bands are to some extent dependent on the neodymium oxide content. Fig. 3 (a) shows the plots of this dependence for the most dominating transitions occurred at 331, 352, 408, 535, 583, 745, 802 and 874 (nm). This figure reveals that the peak height of the absorption coefficient, $\alpha_{max.}$ increases rapidly as the Nd_2O_3 content increases in the glass matrix up to the concentration 4 wt% and then the rate of increase of $\alpha_{max.}$ is generally diminished gradually with the increase of RE oxide content beyond the above content until the end of the investigated range, 8 wt%.

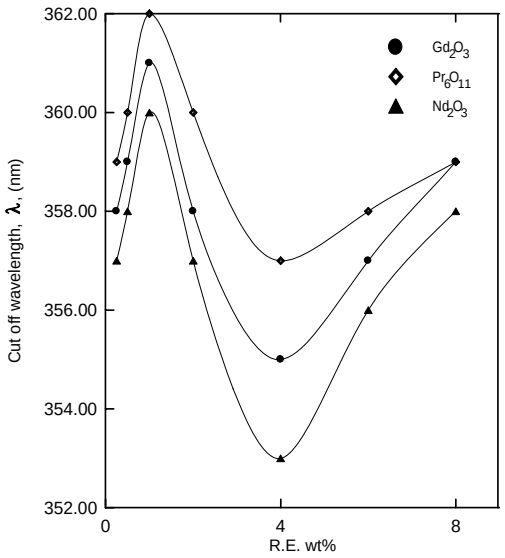

Fig. 3. Variations of the absorbtion band edge wavelength, λ_o, with Re wt % content for $Mn(PO_3)_{4-X}$ Re glasses.

3.2.2. Gd^{3+} ($4F^7$)

The optical properties of Gd^{3+} has been investigated by many authors [26, 32-36]. However, the F-F transitions for, Gd^{3+} ion are weak in comparison with the absorption bands of the glass matrix [26], so that the resulting absorption spectrum has a low signal to noise ratio. Thus, the transition occurs from the $^8S_{7/2}$ ground state level to various excited levels [33, 35]. The dominating transitions are between the $^8S_{7/2}$ ground state level and ^6P_J (J= 7/2, 5/2, 3/2), ^6J_J (J= 15/2 and 13/2) and ^6D_J (J= 3/2 and 5/2) as shown in Fig. 3 (b). Also, the transition wavelengths with their corresponding assignments and their peak absorption coefficient, $\alpha_{max.}$ are given in Table 3. From this Table, it is clear that the values of $\alpha_{max.}$ are dependent on the wt% of the doped Gd_2O_3 oxide. However, Fig. 3 (b) shows this dependence which indicates the appearance of the three composition region through the occurrence of two inflexion points around 1 and 4 wt% of Gd_2O_3 oxide.

Table 2. The values of λ_0, $E_{opt.}$ and ΔE for $Mn(PO_3)_2$. x Nd_2O_3 glasses.

Nd_2O_3 content X(wt %)	λ_0 (nm)	Optical energy $E_{opt.}$ (eV)	Width of band tail ΔE (eV)
0.25	357	2.211	0.652
0.5	358	2.063	0.682
1	360	1.996	0.696
2	357	2.198	0.655
4	353	2.294	0.596
6	356	2.213	0.663
8	358	2.151	0.684

3.2.3. Pr^{3+} ($4F^2$)

For the third tested glass series, which doped with Pr_6O_{11} oxide, the optical properties of Pr^{3+} has been investigated by several authors [10, 27, 37-41]. The Pr^{3+} ion transitions occur from the $^3H_4$ (with total angular momentum J=4) ground state level to various excited levels which attributable to the 4F-4F transitions [40]. The intense of the absorption coefficient, α_{max}, observed at wavelengths below 300nm is due to the 4F-5d transition of Pr^{3+} which makes the predominant contribution to the Faraday rotation in the wavelength range [38]. The absorption bands may be sharp because spin-orbit coupling is quit large and the F orbitals are so well shielded from surroundings of the ions, the various states arising from the $4F^2$ configuration are split only to a small extent [40]. Thus when electronic F-F transitions occur from one J state of the F^2 configuration to another state of this configuration.

Table 3. Absorption spectra of Gd^{3+} in $Mn(PO_3)_2$.x Gd_2O_3 glasses.

Observed Transitions	Wavelength (nm)	α_m(cm^{-1}) for glasses with different values of x						
		0.25%	0.5%	1 %	2 %	4 %	6 %	8 %
$^8S_{7/2}\rightarrow{}^6P_{J\ (J=7/2,5/2,3/2)}$	550	4.54	4.07	3.052.262.87	5.08	7.81	5.72	6.0
$\rightarrow{}^6J_{J\ (J=15/2,13/2,)}$	408	2.54	2.36		3.72	5.16510.32	3.82	2
$\rightarrow{}^6D_{J\ (J=3/2,5/2)}$	350	5	4.36		7.8		6.73	3.3
								6.5

Table 4. The values of λ_0, $E_{opt.}$ and ΔE for $Mn(PO_3)_2.x\ Gd_2O_3$ glasses.

Nd_2O_3 content X(wt %)	λ_0 (nm)	Optical energy $E_{opt.}$ (ev)	Width of band tail ΔE (ev)
0.25	358	2.608	0.472
0.5	359	2.553	0.507
1	361	2.418	0.516
2	358		
4	355	2.585	0.403
6	357	2.5	0.477
8	359	2.35	0.524

Table 5 lists the observed wavelengths with their corresponding attributed transitions and their peak values of, $\alpha_{max.}$. Fig. 3 (c) shows the dependence of $\alpha_{max.}$ with wt% of Pr_6O_{11} oxide content which showed the same trend, i.e. two inflexion points around 1 and 4 wt% of the doped Pr_6O_{11} oxide contents but with converse behavior to that observed for the case of Gd_2O_3 oxide. From this Table, it is clear that, the peaks at 408-480 nm are attributed to the $^3H_4 \rightarrow {}^3P_J$ (J= 0, 1, and 2) and $^1H_6$ transitions and the beaks around 535 nm are $^3H_4 \rightarrow {}^1D_2$ transitions [38, 40] as shown in Fig. 3 (c).

Table 5. Absorption spectra of Pr^{3+} in $Mn(PO_3)_2.x\ Pr_6O_{11}$ glasses.

Observed Transitions	Wave-length (nm)	$\alpha_m(cm^{-1})$ for glasses with different values of x						
		0.25%	0.5%	1 %	2 %	4 %	6 %	8 %
$^3H_4 \rightarrow {}^1D_2$	535	3.51	5.2	5.234.5	4.2	3.77	5.05	8.3
$\rightarrow {}^1I_6$	483	2.6	4.3	63.764.	3.25	2.94	4.66	8.1
$\rightarrow {}^3P_0$	445	1.3	2.04	264.87	2.17	2.04	4.12	6.47
$\rightarrow {}^3P_1$	408	2.13	3.87		2.78	2.1	3.53	6.69
$\rightarrow {}^3P_2$	355	3.81	4.79		3.7	3.6	4.467	8.23

3.3. Optical absorption edge and energy gap of Mn $(PO_3)_4$. x R.E. glasses

Returning to Fig. 2 (a, b and c) which shows the optical absorption spectra for the investigated glasses, $Mn(PO_3)_4.x$ (RE) oxide where RE oxide represents Nd_2O_3, Gd_2O_3 and Pr_6O_{11} respectively, it is seen that there are no sharp absorption edges obtained in these spectra as a result of their glassy state. However, the variations of the fundamental absorption band edge wavelength, λ_0, with the wt% content of RE oxide for all glasses are shown in Fig. 3, which located in the UV region. The plots in this figure reveals the same behavior with two inflexion points around 1 and 4 wt% of RE oxides Nd_2O_3, Gd_2O_3 and Pr_6O_{11} respectively.

The values of the optical energy gap, E_{opt}, and the width of the band tail, ΔE, are obtained using the following formula [32, 42]

$$\alpha(\omega) = B(\hbar\omega - E_{opt.})^2 / \hbar\omega \qquad (2)$$

$$\alpha(\omega) = \alpha_o(\omega)\exp(\hbar\omega / \Delta E) \qquad (3)$$

where $\alpha(\omega)$ is the absorption coefficient, B and α_0 are constants, $\hbar\omega$ is the photon energy and $\hbar$ = h/2π where h is Planck constant.

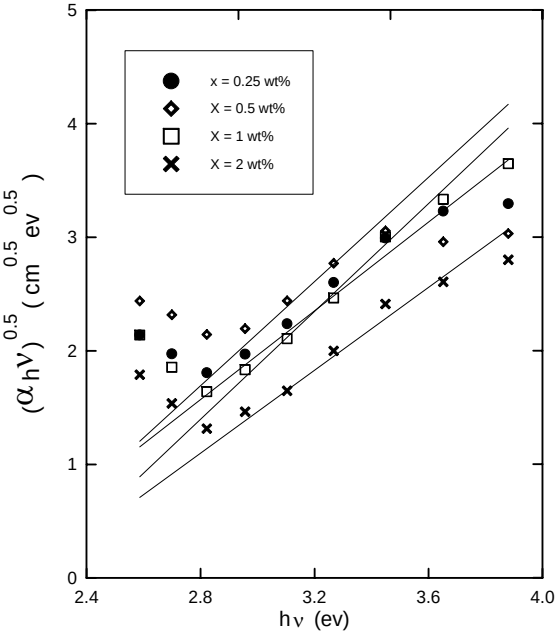

Fig. 4. (a) Variation $(\alpha\hbar\omega)^{1/2}$ with the photon energy, $\hbar\nu$ for $Mn(PO_3)_4.x\ Nd_2O_3$ glasses systems where x = 0.25, 0.5, 1, and 2 wt.%.

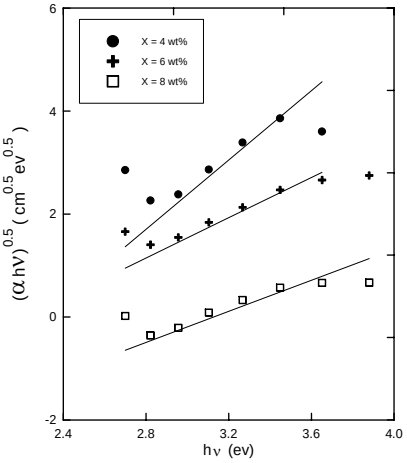

Fig. 4. (b) Variation $(\alpha \hbar\omega)^{1/2}$ with the photon energy, $\hbar\nu$ for $Mn(PO_3)_{4-X}Nd_2O_3$ glasses systems where x = 4, 6 and 8 wt.%.

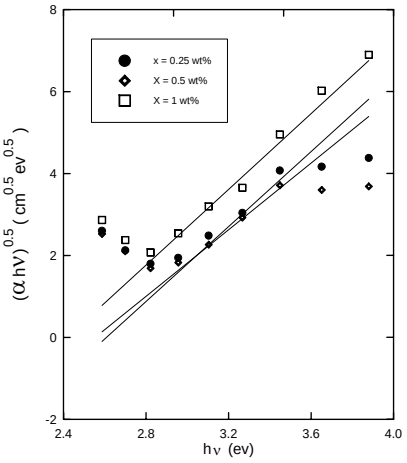

Fig. 5. (a) Variation $(\alpha \hbar\omega)^{1/2}$ with the photon energy, $\hbar\nu$ for $Mn(PO_3)_2.x\ Gd_2O_3$ glasses systems where x = 0.25, 0.5 and 1 wt.%.

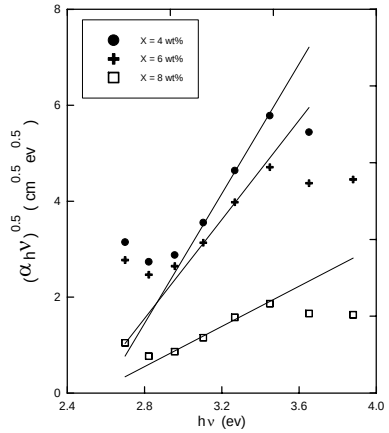

Fig. 5. (b) Variation $(\alpha \hbar\omega)^{1/2}$ with the photon energy, $\hbar\nu$ for $Mn(PO_3)_2.x\ Gd_2O_3$ glasses systems where x = 4, 6, and 8 wt.%.

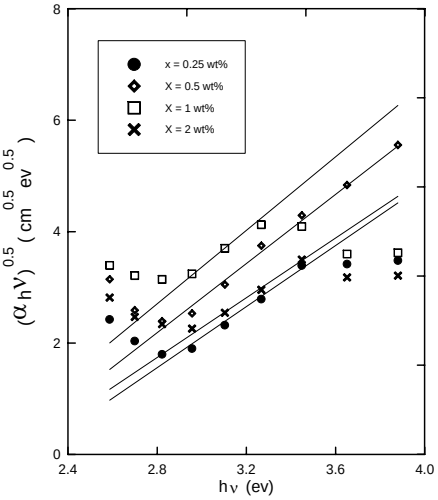

Fig. 6. (a) Variation $(\alpha \hbar\omega)^{1/2}$ with the photon energy, $\hbar\nu$ for $Mn(PO_3)_2.x\ Pr_6O_{11}$ glasses systems where x = 0.25, 0.5, 1, and 2 wt.%.

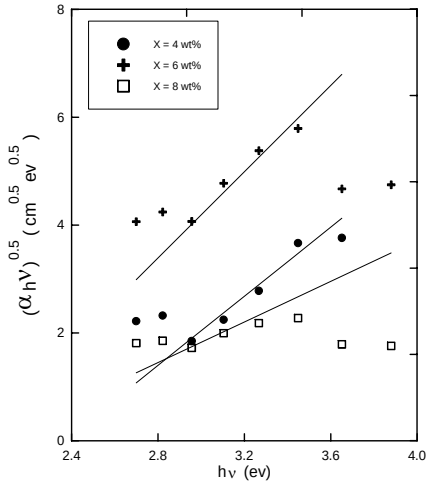

Fig. 6. (b) Variation $(\alpha \hbar\omega)^{1/2}$ with the photon energy, $\hbar\nu$ for $Mn(PO_3)_2.x\ Pr_6O_{11}$ glasses systems where x = 4,6 and 8 wt.%.

The values of the optical energy gap, $E_{opt.}$, are obtained from the extrapolation of the linear part of each curve representing, the variation of the quantity $(\alpha \hbar\omega)^{1/2}$ with the photon energy, $\hbar\nu$, to $(\alpha \hbar\omega)^{1/2} = 0$, (see Figs 4 (a, b), 5 (a, b) and 6 (a, b)) for the manganese-phosphate glasses doped with Nd_2O_3, Gd_2O_3 and Pr_6O_{11} oxides respectively. Also, the width of the band tail of the localized states, ΔE, is obtained for all glasses, according to equation (3) from the slope of each plot respecting the variation of $\ln\alpha$ with $\hbar\nu$ (see Figs. 7 (a, b), 8 (a, b) and 9 (a, b)) for the above mentioned glasses, respectively. The obtained values for both $E_{opt.}$ and ΔE for the investigated glasses are given in Tables (2, 4 and 6). Dependences of $E_{opt.}$ and ΔE on the wt% content of the doped RE oxide are shown in Fig. 10 (a and b), respectively. Inspection of this

figure reveals that, the optical energy gap and the width of the band tail have a inverse compositional dependence on the R.E. oxide content for all tested glasses. The appearance of the inflexion points at 1 and 4 wt% of RE oxide content (Fig. 10) indicates the occurrence of some structural changes in the prepared glasses network, which led to the obtaining of the three regions, 0.25~1, 1~4 and 4~8 wt% of doping RE oxide. However, effects of these structural changes on the optical absorption edge, λ_0, (Fig. 4) and optical energies, $E_{opt.}$ and ΔE (Fig. 10) or the compositional dependence of these quantities could be understood as follows; In the first compositional region, from 0.25~1 wt% content of RE oxide, the effect of the addition of these doped RE cations is to breakdown the network bonds, P-O-P and Mn-O-P for entire vitreous range of the studied glasses, so that the absorption band edge wavelength, λ_0, will be shifted to longer wavelengths (i.e. lower photon energies) leading to a decrease in the values of, $E_{opt.}$, and an increase in the values of ΔE. Increasing the RE cations in the second region of composition (1-4 wt%), this may allow the doped R.E cations to enter into the glass network forming positions of $Mn(PO_3)_4$ [13], which, increase the degree of cross-linking. This leads to the observed shift of the absorption edge wavelength, λ_0, to lower values (or higher photon energies). Therefore, the optical energy gap is increased and the width of the band tail is decreased as shown in the above mentioned Figures. Beyond 4 wt% of the RE content, the addition of RE cations increases the number of non-bridging oxygen atoms as these RE cations reside in the glass structure interstitially. Thus the absorption band edge wavelength, λ_0, shifts to longer wavelengths (i.e. lower energies) as shown in Fig. 4, so that the optical energy gap is decreased and the width of band tail increased as shown in Fig. 10. This is in accordance with Steveel's suggestion [43], which involves that, the shift of UV absorption band to longer wavelengths corresponds to transitions from the non-bridging oxygen which bind an excited electron less tightly than a bridging one and lead to a decrease in the value of, $E_{opt.}$ and an increase in that of ΔE. So according to Stevels suggestion one can argue that the observed variations of, $E_{opt.}$, and , ΔE, beyond 4 wt. % may be due to an increase in the number of non-bridging oxygen atoms.

Table 6. The values of λ_0, $E_{opt.}$ and ΔE for $Zn(PO_3)_2$. x Pr_6O_{11} glasses.

Nd_2O_3 content x(wt %)	λ_0 (nm)	Optical energy $E_{opt.}$ (ev)	Width of band tail ΔE (ev)
0.25	359	2.231	0.4
0.5	360	2.1	0.438
1	362	1.95	0.61
2	360	2.1	0.503
4	357	2.363	0.364
6	358	2	0.531
8	359	1.94	0.541

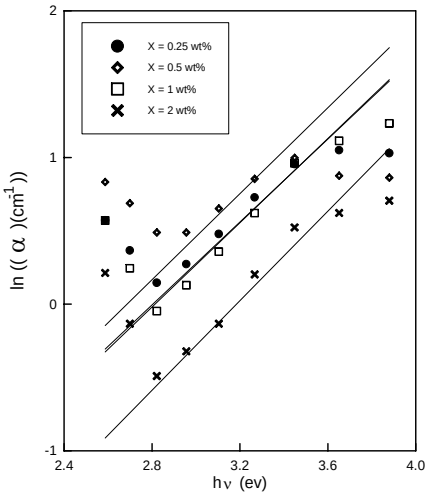

Fig. 7. (a) Variation lnα with the photon energy, $\hbar\nu$ for $Mn(PO_3)_{4-X}Nd_2O_3$ glasses systems where x = 0.25, 0.5, 1 and 2 wt.%.

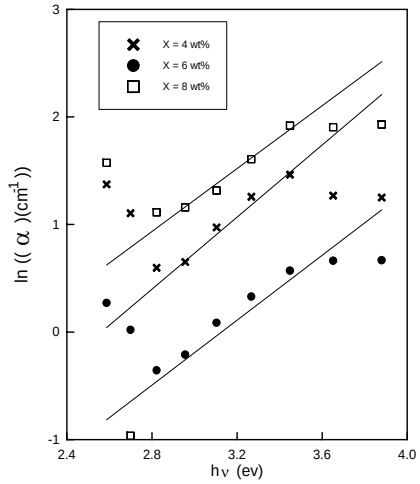

Fig. 7. (b) Variation lnα with the photon energy, $\hbar\nu$ for $Mn(PO_3)_{4-X}Nd_2O_3$ glasses systems where x = 4,6 and 8 wt.%.

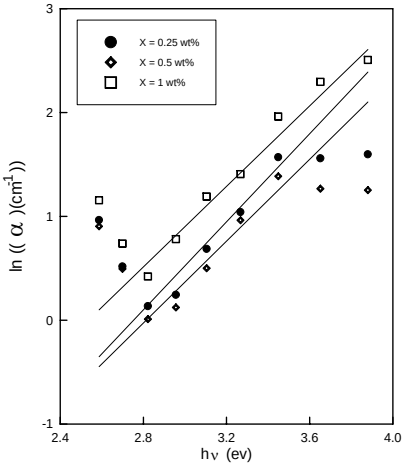

Fig. 8. (a) Variation lnα with the photon energy, $\hbar\nu$ for $Mn(PO_3)_{4-X}Gd_2O_3$ glasses systems where x = 0.25, 0.5, and 1 wt.%.

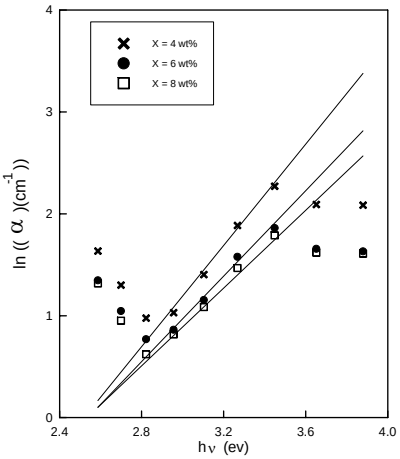

Fig. 8. (b) Variation lnα with the photon energy, ħν for $Mn(PO_3)_{4-X}Gd_2O_3$ glasses systems where x = 4, 6 and 8 wt.%.

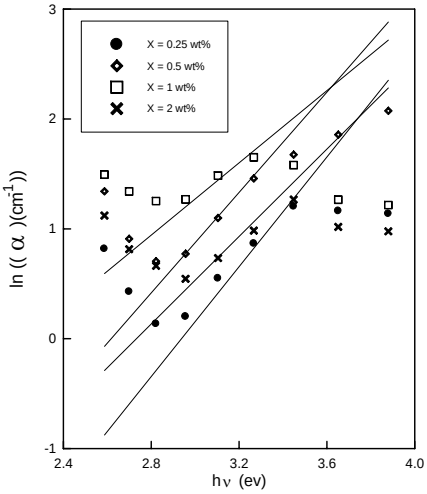

Fig. 9. (a) Variation lnα with the photon energy, ħν for $Mn(PO_3)_{4-X}Pr_6O_{11}$ glasses systems where x = 0.25, 0.5, 1 and 2 wt.%.

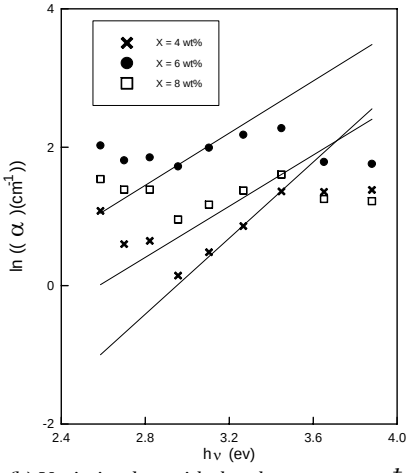

Fig. 9. (b) Variation lnα with the photon energy, ħν for $Mn(PO_3)_{4-X}Pr_6O_{11}$ glasses systems where x = 4, 6 and 8 wt.%.

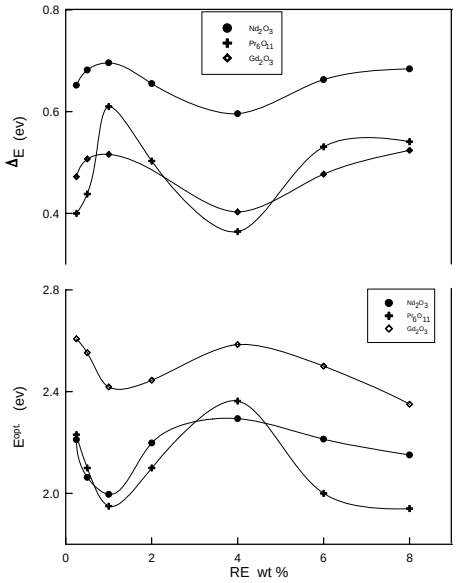

Fig. 10. Variations of (a) $E_{opt.}$ and (b) ΔE with RE wt% $Mn(PO_3)_{4-X}$ RE glasses systems (where RE are Nd_2O_3) or Gd_2O_3 or Pr_6O_{11}).

4. Conclusions

The present studies indicated that the values of $E_{opt.}$ were calculated for n = 2 i.e. indirect transitions and the values of ΔE were obtained from Urbach edge. The absorption band edge wavelength (λ_0), $E_{opt.}$ and ΔE are found to be strongly dependent on R.E. oxide content. Also the maximum values of the absorption coefficient for the observed absorption bands, $\alpha_{max.}$, are found to be compositional dependent. The compositional dependence in the present investigations shows three distinct compositional regions around 1 and 4 wt. % R.E oxide content. The number of breaks depends on the kind of the rare-earth oxides, but the intensity of breaks are different.

References

[1] R. Reisfeld, C. K. Jorgensen, Lasers and excited states of rare earths, Springer, Berlin (1977).
[2] Aggarwal, G. Lu, eds., Fluoride glass fiber optics, Academic press, San Diego CA (1991).
[3] S. Ray Bullock, B. R. Reddy, Carlton L. Pope, S. K. Nash- Stevenson, J. Non. Cryst. Solids **212**, 85-88 (1997).
[4] Y. Jiang, S. Jiang, Y. Jiang, J. Non Cryst. Solids 286 (1989).
[5] M. J. Weber, J. Non-Cryst. Solids **113**, 208 (1990).
[6] W. Krupke, IEEE J. Quantum Electron. Q E –**7**, 153 (1971).
[7] M. J. Weber, T. E. Varitimos, J. Appl. Phys. **42**, 4996 (1971).
[8] T. S. Lombeim, L. G. De Shazer, J. Appl. Phys. **49**, 5517 (1978).
[9] E. Culea, I, Milea, J. Non-Cryst. 189 (1995).
[10] B. C. Joshi, M. C. Joshi, J. Non-Cryst. Solids

142, 171 (1992).
[11] M. N. Khan, Ravisankar Harani, M. M. Ahmed, C. A. Hogarth, J. Mat. Sci. **20**, 2207 (1985).
[12] D. Guillet-Noel, B. Bellany, B. Viana, D. Gourier,. Phys. Rev. B **6**(3), 1668 (1999).
[13] M. J. Weber, R. A. Saroyan, R. C. Ropp, J. Non Cryst. Solids, **44**, 137 (1981).
[14] S. Tanabe T. Hanada, T. Ohyaygi N. Soga, Phys. Rev. B **48**, 10591 (1993).
[15] J. Obyun B. H. Hin, K. S. Hong, H. J. Jung, S. W. Lee, K. S. Ryoo, A. A. Izaneev, V. B. Kravchenko, Jpn. J. Appl. Phys. **33**, 4907 (1994).
[16] G. Ajith Kumar, P. R. Biju, C. Venugopal, N. V. Unnikrishnan, J. Appl. Phys. **221**, 47 (1997).
[17] A. S. El-Joundi, A. A. Higazy, Indian J. Phys. **70A** (5), 581 (1996).
[18] M. Syczewski, K. Wieczffinski, Am. Soc. Chim. Polonorum **49**, 1059 (1975).
[19] R. Reisfeld, Structure and Bonding **13**, 53 (1973).
[20] N. B. BrachJkovskaya, S. G. Lunter, A. K. Przhevuskii, E. L. Raaben, M.. N. Tolstoi, Opt. Spectr. (USSR) **43**, 411 (1977).
[21] M. J. Weber, R. A. Saroyan, J. Non Cryst. Solids **44**, 137 (1981).
[22] C. A. Hogarth, M. A. Ghauri, J. Mater. Sci. **14**, 1641 (1979).
[23] J. D. Mackenzie, 'Modern Aspects of the Vitreous State' Vol. II (Butter Worths, London, 1964) P. 126.
[24] Z. Konstants, M. Vaivada, J. Non-Cryst. Solids **45**, 105 (1981).
[25] C. E. Deshprandhe, S. K. Date, J. Mat. Sci. Let. **3**, 563 (1984).
[26] K. Binnemans, R. Van Deun, C. Görller-Walrand, J. L. Adam, J. Non-Cryst. Solids **238**, 11 (1998).
[27] Ravishankok Harani, C. A. Hogarth, M. M. Ahmed, D. F. C. Morris, J. Mat. Sci. Let. 3, 843 (1984).
[28] B. Sharma, D. K. Rai, S. B. Rai, Indian J. Phys. **70** B (5), 397 (1996).
[29] E. U. Condon, G. H. Shortly, The Theory of Atomic Spectra, Cambridge University Press, Cambridge (1935).
[30] A. H. Khafagy, S. M. El-Rabie, A. A. Higazy, A. S. Eid Indian J. Phys. **74A**(4), 433 (2000).
[31] K. N. R. Taylor, M. I. Barby, Physics of Rare Earth Solids, Chapman and Hall Landon (1972).
[32] N. F. Mott, E. A. Davis, Electronic Processes, in Non-Crystalline Materials. Oxford Univ. Press, Oxford (1979).
[33] M. N. Khan, Ravisankar Harani, M. M. Ahmed, C. A. Hogarth, J. Mat. Sci. **20**, 2207 (1985).
[34] R. P. Khare, J. D. Ranade, J. Mat. Sci. Let. **15,** 1868 (1980).
[35] M. Bouazaoui, B. Jacquier, C. Linares, W. Strek, J. Phys. Cond. Matt. **3**, 921 (1991).
[36] Taiju Tsuboi, J. Phys. Condens. Matt. **10**, 9155 (1998).
[37] M. M. Ahmed, R. Harani, C. A. Hogarth. J. Mat. Sci. Let. **3**, 1055 (1992).
[38] Y.C. Ratnakaram, N. Sudharani, S. Buddhudu, Indian J. Phys. **70** B(5), 409 (1996).
[39] J. E. Munoz-Santiuste, A. Lorenzo, L. E. Bausa, J. Gorcia Sole, J. Phys. Cond. Matt. **10**, 7653 (1998).
[40] Katswhisa Tanaka, Neoki Tatehata, Koji Fujita, Kazuyuki Hiroo, J. Phys. B. Appl. Phys. **31**, 2622 (1998).
[41] J. L. Adam, W. A. Siblds, J. Non-Cryst. Solids **76**, 267 (1985).
[42] G. W. Anderson, W. D., J. Compton, Chem. Phys. **52**, 6166 (1970).
[43] J. M. Stevels, 11th Int. Cong. On "Pure and Applied Chemistry " **5**, 519 (1953).